IEEE Access
Multidisciplinary | Rapid Review | Open Access Journal

Received September 4, 2018, accepted October 2, 2018, date of publication October 11, 2018, date of current version October 29, 2018.

Digital Object Identifier 10.1109/ACCESS.2018.2874812

An Active Contour Model Based on Region Based Fitting Terms Driven by p-Laplace Length Regularization

SHAFIULLAH SOOMRO[1], (Member, IEEE), TOUFIQUE AHMED SOOMRO[2], (Member, IEEE), AND KWANG NAM CHOI[3], (Member, IEEE)

[1]Quaid-e-Awam University of Engineering Science and Technology, Larkana 77150, Pakistan
[2]School of Computing and Mathematics, Charles Sturt University, Sydney, NSW 2795, Australia
[3]Department of Computer Science and Engineering, Chung-Ang University, Seoul 156-756, South Korea

Corresponding author: Kwang Nam Choi (knchoi@cau.ac.kr)

This work was supported by the Basic Science Research Program through the National Research Foundation of Korea (NRF) funded by the Ministry of Education, Science and Technology under Grant NRF-2010-0025512.

ABSTRACT In this paper, we propose a partial differential equation structure that permits an active contour method to obtain intensity inhomogeneous image segmentation. We consider fitted model comprised of local and global energy functions dictated by the scaled p-Laplace term acting as a length regularization term. A new local model is formulated by taking bias field into the local fitted model, which improves the performance of the proposed method relatively. The scaled p-Laplace equation exhibited as a regularized length term, which is utilized to reduce the impact of noise over level set minimization while guaranteeing the curve not to go through feeble boundaries. Inhomogeneities comprise of unwanted pixel variations called bias field, which change the consequences of the level set-based methods. Thereby, Gaussian distribution is used for the approximation of the bias field, and further bias field is used for bias correction likewise. Moreover, local model has been remodeled by integrating bias field inside their local information; similarly, global model is also established on the pretext of the local model. At last, we demonstrate the results on some complex images to show the strong and exact segmentation results that are conceivable with this new class of dynamic active contour model. We have also performed statistical analysis on mammogram images using accuracy, sensitivity, and Dice index metrics. Results show that the proposed method gets high accuracy, sensitivity, and Dice index values compared to the previous state-of-the-art methods.

INDEX TERMS Active contours, bias field, level set, p-Laplace.

I. INTRODUCTION

Active contour image segmentation strategies have turned out to be extremely famous, and have discovered applications in a variety of issues including visual tracking and image segmentation [1]. The essential thought is to permit a curve to deform by minimizing a given energy functional to accomplish desired segmentation result. Two major classes exist for active contours: edge-based and region based.

Edge-based active contours use gradient image information to recognize object boundaries [2]–[4]. This type of gradient data is sufficient in a few circumstances. However, has been observed to be extremely delicate to noisy images and exceptionally reliant on initialization curve position. One advantage of this kind of scheme is that no region imperatives are put on an image. Therefore, the right segmentation can be accomplished in certain cases for heterogeneous or homogeneous background images.

On the contrary, work in region-based active contours have been centered around region based streams inside an image [5]–[22]. These methodologies demonstrate the foreground and background measurably and establish an energy function that best fits the image. Among all-region based methods portion of the broadly utilized region-based models are global which assume the image regions to be constant or homogeneous [5], [6]. Similarly, Some of the notable region-based models are local, which overcome the constraints of the global techniques and consider image local information to carry out intensity inhomogeneous segmentation [12]. The comparison result of edge and region base segmentation is shown in Fig 1, where (a) shows the result of LSEWR

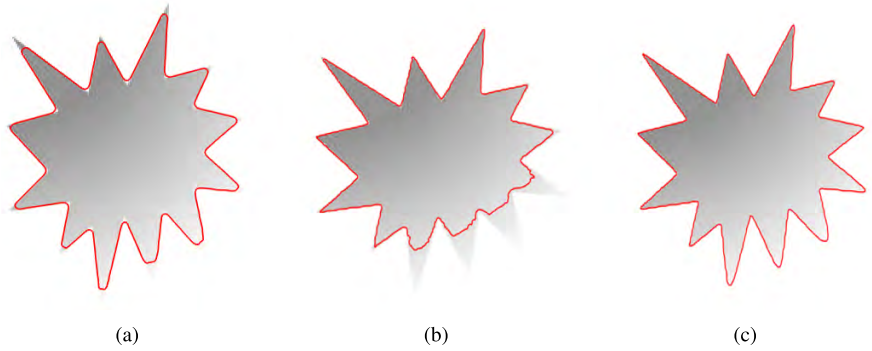

FIGURE 1. Image segmentation using previous methods a: Segmentation result of the LSEWR [4] method. b: Segmentation result of Chan and Vese [6] method. c: Segmentation result of the LBF [12] method.

(level set evolution without re-initialization) [4] method, (b) shows the result of the Chan and Vese [6] and (c) shows the result of the LBF (local binary fitting) [4] method. It can be deduced from Fig 1 that, local region based methods have some capability to handle intensity inhomogeneities to some extent. However, local region based methods are not always sufficient to carry out an accurate image segmentation.

Regardless of numerous intensity-based segmentation methods, the segmentation of the intensity inhomogeneous images is still an existing issue in image segmentation, which emerges from substandard image procurement process or because of outside impedance. It has been analyzed that Bias field is also used as an initial step for accomplishing better segmentation results. In this regard, bias correction based active contour methods [23]–[25] are the most adaptable because these methods are using a unified structure of performing segmentation with bias correction. A unified local energy model was proposed by Zhang et al. [14]. In this method, local image fitting (LIF) energy model is characterized by using image local information. This information adapted to build up a differential model between the original image and fitted image. Moreover, another technique is utilized to regulate the level-set function stability by utilizing Gaussian kernel after every cycle.

Li et al. [23], [26] proposed a level-set segmentation method (VLSBCS) using bias correction for images defiled with intensity variations or inhomogeneity. This model has characterized an energy functional that partition an image domain and calculates bias field in a level set framework. The minimization of the energy functional performs segmentation and bias field estimation together. Moreover, the slowly varying property of the bias field is ensured by the data term without the involvement of smoothing term.

More recently hybrid active contour models [8]–[11], [18] have been very popular for image segmentation. These models combine region and edge information in a different way based on different applications. Soomro et al. [9] proposed a two-stage hybrid method, which integrates region and edge information in two stages. First stage of this method uses global region with edge information which produces rough segmentation results, in the second stage local region information is combined with edge information to produces final segmentation result.

Recently, p-Laplace based level set image segmentation strategy is anticipated in [27]. A weighted p-Laplace integral is used as a geometric length regularization term, which is utilized to reduce the impact of noise during curve minimization. The thought behind the new energy functional is that the measure of regularization on the level set can be balanced by p-Laplace term.

In this research, we propose a novel active contour method with following contributions.

1) A novel fitted model is formulated, which combines local and global information. Local fitted model assists moving contour to fragment objects with inhomogeneity and global fitted model speeds up the contour movement over constant intensity regions.
2) Bias field has been taken into consideration for local fitted model, which increases the accuracy of the proposed method.
3) p-Laplace integral is used as length regularization term. It provide smooth contours and prevent level set to produce unnecessary contours during curve evolution.

After implementing proposed method, we performed investigations with both real and synthetic images to show that the current technique yield better outcome and provide more details with bias-corrected image than previous methods.

The subsequent steps are arranged as follows. The background explanations are described in section II. The proposed research is explained in section III. Experimental and comparison analysis are depicted in section IV. Quantitative validations are presented in section V using mini-Mias dataset. Discussion is presented in section VI. At last, the conclusion is described in section VII.

II. BACKGROUND

A. MUMFORD AND SHAH MODEL

Mumford and Shah [5] anticipated a region-based image segmentation method. This technique characterizes an optimal

approximation function μ of the image I. Piecewise approximation function changes smoothly inside a sub-region of image domain $I : \Omega \subset R^2$. The anticipated energy functional is written as:

$$E_{MS} = \lambda \int_{\Omega} (I(x) - \mu(x))^2 + v \int_{\Omega \setminus C} (\nabla \mu(x))^2 dx + \mu \int_{\Omega} L(C) \tag{1}$$

$L(C)$ is curve length, μ and v are constant parameters. It has been observed that the energy of Mumford and Shah model owns non-convex performance and the non-regularity of the edge term creates trouble through energy minimization process.

B. Chan-Vese MODEL

Chan and Vese [6] anticipated a more comprehensible energy functional grounded on the concept of Mumford and Shah model [5]. By approximating the image intensities inside and outside of contour, Chan-Vese calculates average intensities known as j_1 and j_2 respectively. Let an input image is represented as $I : \Omega \subset R^2$, level set function $\phi : \Omega \subset R^2$ and contour C is implicitly represented with zero level set: $C = \{x \in \Omega | \phi(x) = 0\}$. The energy of Chan-Vese method mathematically written as follows:

$$\begin{aligned} E_{CV}(C, j_1, j_2) = \lambda_1 &\int_{\Omega} |I(x) - j_1|^2 H_\varepsilon(\phi(x)) dx \\ &+ \lambda_2 \int_{\Omega} |I(x) - j_2|^2 (1 - H_\varepsilon(\phi(x))) dx \\ &+ \mu \int_{\Omega} |\nabla H_\varepsilon(\phi)|^2 dx + v \int_{\Omega} H_\varepsilon(\phi) dx \end{aligned} \tag{2}$$

where some scaling constants are $\mu \geq 0$, $v \geq 0$ and $\lambda_1, \lambda_2 \geq 0$, where $\mu \geq 0$ balances the length term and v balances the area term for curve C respectively. $H_\varepsilon(\phi)$ is the standardized Heaviside function written as:

$$H_\varepsilon(\phi) = \frac{1}{2}\left(1 + \frac{2}{\pi} \arctan\left(\frac{\phi}{\varepsilon}\right)\right) \tag{3}$$

ϵ balances the smoothness of Heaviside function. Two constants j_1 and j_2 in Eq (2), characterize global region intensities within both sides of curve C. By getting derivative of Eq (2), with respect to ϕ by means of gradient descent technique [28], the equivalent level set formulation is written as follows.

$$\frac{\partial \phi}{\partial t} = \left(-\lambda_1 (I - j_1)^2 + \lambda_2 (I - j_2)^2 + \mu div\left(\frac{\nabla \phi}{|\nabla \phi|}\right) - v\right) \delta_\varepsilon(\phi) \tag{4}$$

$\delta_\epsilon(\phi)$ is a smooth version of a Dirac delta function, which is defined as:

$$\delta_\varepsilon(\phi) = \frac{\varepsilon}{\pi(\phi^2 + \varepsilon^2)} \tag{5}$$

Alongside scaling the smoothness of a Heaviside function in Eq (3), ϵ likewise balances the width of a Dirac delta function in Eq (5). Keeping ϕ fixed and minimizing energy in Eq (2), with respect to j_1 and j_2, we get the following formulations:

$$\begin{aligned} j_1 &= \frac{\int_{\Omega} I(x) H_\varepsilon(\phi(x)) dx}{\int_{\Omega} H_\varepsilon(\phi(x)) dx} \\ j_2 &= \frac{\int_{\Omega} I(x)(1 - H_\varepsilon(\phi(x))) dx}{\int_{\Omega} (1 - H_\varepsilon(\phi(x))) dx} \end{aligned} \tag{6}$$

The energy functional in Chan-Vese technique is associated with global intensity characteristic of an image region within both sides of curve C. Consequently, this method produces an improper result if the image has local or inhomogeneous intensity regions.

C. LOCAL BINARY FITTED MODEL

Li et al. [12] anticipated local binary fitted (LBF) technique to deal with intensity inhomogeneity problem by coupling local image information into their energy functional. Let we assume an image $I : \Omega \subset R^2$, a level set $\phi : \Omega \subset R^2$, and closed contour as C. The proposed energy formulation is defined as:

$$\begin{aligned} &E_{LBF}(C, f_1, f_2) \\ &= \lambda_1 \int_{\Omega} K_\sigma(x - y) |I(y) - f_1(x)|^2 H_\epsilon(\phi(y)) dy \\ &\quad + \lambda_2 \int_{\Omega} K_\sigma(x - y) |I(y) - f_2(x)|^2 (1 - H_\epsilon(\phi(y))) dy \end{aligned} \tag{7}$$

where some scaling values are λ_1, $\lambda_2 \geq 0$ and $H_\varepsilon(\phi)$ is the standardized Heaviside function explained in Eq (3). $f_1(x)$ and $f_2(x)$ are local means calculated from both sides of curve C defined as.

$$f_1(x) = \frac{K_\sigma * [H_\epsilon(\phi) I(x)]}{K_\sigma * H_\epsilon(\phi)} \tag{8}$$

$$f_2(x) = \frac{K_\sigma * [(1 - H_\epsilon(\phi)) I(x)]}{K_\sigma * (1 - H_\epsilon(\phi))} \tag{9}$$

Distance regularization term from [4] is merged in to Eq (7) to guarantee stable outcome. Additionally, the length term is also integrated for level set regularization ϕ. The mathematical formulation of this technique is written as:

$$\begin{aligned} \frac{\partial \phi}{\partial t} &= -\delta_\varepsilon(\phi) \lambda_1 \int_{\Omega} K_\sigma(x - y) |I(x) - f_1(y)|^2 dy \\ &\quad - \lambda_2 \int_{\Omega} K_\sigma(x - y) |I(x) - f_2(y)|^2 dy (-\delta_\varepsilon) \\ &\quad + v \delta_\varepsilon(\phi) div\left(\frac{\nabla(\phi)}{|\nabla(\phi)|}\right) + \mu\left(\Delta\phi - div\left(\frac{\nabla \phi}{|\nabla \phi|}\right)\right) \end{aligned} \tag{10}$$

In above equation, μ represent scaling value for distance regularized penalty term and v shows constant parameter for length term, which initiatives the movement of curve to object

boundaries. K_σ is a Gaussian window function with standard deviation defined as:

$$K_\sigma(x-y) = \frac{1}{(2\pi)^{n/2}\sigma^n}\exp\left(-\frac{|x-y|^2}{2\sigma^2}\right) \quad (11)$$

σ represents standard deviation of the Gaussian function, which balances the localization property of LBF model i-e., from small neighborhood to whole image domain. The inclusion of Gaussian function contemplates an image local intensity information within both sides of contour C and permit this technique to capture objects with intensity inhomogeneity. Nevertheless, local intensity information is not always enough to carry out an precise segmentation. Furthermore, this method is awfully subtle to the position of initialization curve and jammed into local minima if we place initial contour away from boundaries.

D. LOCAL IMAGE FITTED (LIF) MODEL

Local Image fitting (LIF) model was proposed in [14], which uses fitted model in their energy functional by taking the subtraction between original image and fitted image. The energy of this method is defined as bellow.

$$E_{LIF} = \frac{1}{2}\int_\Omega |I(x) - I_{LIF}(x)|^2 dx, \quad (12)$$

I_{LFI} is locally fitted image defined as:

$$I_{LIF}(x) = f_1(x)H_\epsilon(\phi) + f_2(x)(1 - H_\epsilon(\phi)) \quad (13)$$

f_1 and f_2 are locally approximated intensities defined in Eq (8) and Eq (9). $H_\epsilon(\phi)$ is Heaviside function defined in Eq (3). Using gradient descent method [28], minimization of Eq (12) with respect to ϕ yields following formulations.

$$\frac{\partial\phi}{\partial t} = (I(x) - I_{LIF}(x))(f_1(x) + f_2(x))\delta_\varepsilon(\phi) \quad (14)$$

E. VLSBCS MODEL

Recently, Li et al. [23], [26] proposed a method for intensity inhomogeneous images known as (VLSBCS) variational level-set method for the segmentation and bias correction. This method computes bias field and guarantees to be smooth over the data term. This method depends on retinex model, which demonstrate images having intensity variations or inhomogeneities this model characterized as:

$$I(x) = b(x)J(x) + n(x), \quad (15)$$

In above equation, *I(x)* shows an intensity inhomogeneous image, *J(x)* is the image to be re-established as free from inhomogeneities, *b(x)* is the bias field that is responsible for intensity variations or inhomogeneities and *n(x)* is noise. This method presumes restored image *J(x)* as constant within every object inside an image. This concept mathematically visualized as:

$$J(x) \approx \sum_{i=1}^{N} c_i M_i \quad for \quad x \in \Omega_i \quad with\, x \in \{\Omega_i\}_{i=1}^N, \quad (16)$$

This method uses K-means clustering to classify local image intensities. K-means utilize iterative procedure to minimize following objective function:

$$E \cong \int \left(\sum_{i=1}^{N}\int_{\Omega i} K_\sigma(x-y)|I(y) - b(x)c_i|^2 dy\right)dx \quad (17)$$

In above equation $b(x)$ is the bias field and c_i represents intensity means. The value of i will be $(i = 1, 2)$ for single level set active contour model. Moreover, $b(x)c_i$ can be characterized as the estimation of the means m_i of the clusters in proportion to each phase of the single level set active contour method. In the case of two-phase active contours, minimizing the above formulation with respect to partition $\{\Omega_i\}_{i=1}^N$. We have two regions Ω_1, Ω_2 represented by zero level set such that $\Omega_1 \cong \phi > 0$ and $\Omega_2 \cong \phi < 0$. We have corresponding energy functional:

$$E = \int \left(\sum_{i=1}^{N}\int_{\Omega i} K_\sigma(x-y)|I(y) - b(x)c_i|^2 M_i(\phi) dy\right)dx, \quad (18)$$

Where M_i is characteristic function based on standardized Heaviside function, for two-phase level set method $M_1 = H(\phi)$ and $M_2 = (1 - H(\phi))$. By getting the first order differential derivative of E, we get the undermentioned functions for $b(x)$ and c_i.

$$b(x) = \frac{\sum_{i=1}^{2} K_\sigma * \left[I(x)c_i M_i(\phi)\right]}{\sum_{i=1}^{2} K_\sigma * \left[c_i^2 M_i(\phi)\right]} \quad (19)$$

$$c_i = \frac{\int K_\sigma * \left[I(x)b(x)M_i(\phi)\right]dx}{\int K_\sigma * \left[b^2(x)M_i(\phi)\right]dx} \quad (20)$$

F. ZHOU et al MODEL

Zhou and Mu [27] proposed another level set boundary extraction technique whose movement is administered by p-Laplace term. The final energy function of this method is characterized as:

$$E(\phi) = \lambda_d E_d(\phi) + \lambda_c E_c(\phi) + \lambda_l E_l(\phi) \quad (21)$$

where λ_d, λ_c and λ_l are constant parameters. In above equation, $E_d(\phi)$ is a regularization term taken from LSEWR [4], which is used to prevent level set from being too flat or steep, $E_c(\phi)$ is energy which drives the motion of the contour to extract object and $E_l(\phi)$ is p-Laplace equation, which provides smoothness and avoids the occurrence of unnecessary contours. The formulations in Eq (21) are further defined as:

$$E_d(\phi) = \frac{1}{2}\int_\Omega (\nabla\phi - 1)^2 d\Omega \quad (22)$$

$$E_c(\phi) = \int_\Omega H(-\phi)|\nabla\phi|^2 d\Omega \quad (23)$$

$$E_l(\phi) = \int_\Omega \delta(\phi)|\nabla\phi|^p d\Omega \quad (24)$$

Minimization of Eq (21) with respect to ϕ, the final level set equation of this method is defined as:

$$\frac{\partial \phi}{\partial t} = \lambda_d\left[\Delta\phi - div\left(\frac{\nabla\phi}{|\nabla\phi|}\right)\right] + \lambda_c\left[\delta(\phi)|\nabla\phi|^2 + 2div\left[H(-\phi)\nabla\phi\right]\right] + \lambda_l\delta(\phi)div\left(|\nabla\phi|^{p-2}\nabla\phi\right) \quad (25)$$

This method handles topological changes smoothly and produces better results. However, this method is not able to segment objects with inhomogeneities.

III. PROPOSED METHOD

The proposed model is inspired from retinex model explained in Eq (15), where $J(x)$ is thought to be established by smooth image components i-e., k. $I(x)$ would thus be depicted as:

$$I(x) = b(x)\{c_1M_1 + c_2M_2 + ...c_kM_k\} \quad (26)$$

where intensity means c_i calculated for corresponding region $\{\Omega_i\}_{i=1}^N$ and M_i is the characteristic function of every region.

The proposed level set formulation is defined by,

$$E_{p,LGFI} = \alpha E_{LGFI}(\phi) + \mu L_p(\phi) + vA(\phi) \quad (27)$$

where $E_{LGFI}(\phi)$ is local and global fitted force term, which operates the movement of the level set function. α, μ and v are fixed parameters. $L_p(\phi)$ is weighted p-Laplace length regularization term [14] defined as:

$$L_p = \mu\int_\Omega \delta(\phi)|\Delta\phi|^p d\Omega \quad (28)$$

where p is a constant value chosen between 1 or 2, which is determined by the image we are dealing. With the help of weighted p-Laplace integral regularization, proposed method can capture obscured boundaries and stop the appearance of false contours during energy minimization, which was previously not possible by using traditional edge indicator function. In Eq (27), $A(\phi)$ is the area term that speed up the curve evolution process defined as.

$$A(\phi) = \int H_\epsilon(-\phi) \quad (29)$$

In Eq (27), we propose an external energy E_{LGFI} supported on local and global fitted image models. Local model is improved by integrating bias field inside the LIF [14] formulation. Similarly, global model is also established by using global means into the LIF [14] model instead of local. The E_{LGFI} model is defined as:

$$E_{LGFI} = \int_\Omega w(I(x)-I_{bLFI}(x))^2 + (1-w)(I(x)-I_{GFI}(x))^2 dx \quad (30)$$

The scaling parameter w is utilized to adjust the model for different kinds of images. w is chosen near to 1 if an image has more intensity variations or inhomogeneities and w is chosen near to 0 for images, which have smooth or homogenous regions. I_{bLFI} accounts for local fitted image and I_{GFI} for global fitted image model defined as:

$$E_{bLFI} = b(x)(c_1M_1 + c_2M_2) \quad (31)$$

$$E_{GFI} = (j_1M_1 + j_2M_2) \quad (32)$$

where local means are represented as c_1 and c_2 and global means as j_1 and j_2 as characterized in Eq (20) and Eq (6). Moreover, the characteristic function is represented as standardized Heaviside function from Eq (3) i.e $M1$ and $M2$, defined as, $M1 = H(\phi)$ and $M2 = (1 - H(\phi))$.

Models using only global force are not adequate to carry out segmentation with intensity inhomogeneity. On the other, models based on the only local force have a higher time complexities. Utilizing both local and global fitted force terms, the proposed technique can handle the intensity inhomogeneity issue with less time complexity. Further, it has been also observed that models with energy functional using only global fitted model can't capture images with inhomogeneity because global models are established under the assumption of homogeneous intensity information. The visual representation of the proposed method is demonstrated in Fig 2, which describes the way local and global information (column 3) is considered by the proposed method compliance with bias field estimation (column2).

By utilizing gradient descent method [28], E_{LGFI} in Eq (27) is minimized with respect to ϕ, we have following formulations:

$$\frac{\partial \phi}{\partial t} = w(b(x)(I(x) - I_{LIF}(x))(c_1(x) + c_2(x))\delta_\varepsilon(\phi)) + (1-w)((I(x) - I_{GFI}(x))(j_1(x) + j_2(x))\delta_\varepsilon(\phi)) + \mu\delta(\phi)div(|\Delta\phi|^{p-2}\Delta\phi) - v\delta(\phi) \quad (33)$$

Where bias approximated field is represented as $b(x)$ used in Eq (19), and j_1, j_2 are global intensity averages taken from Eq (6) and local intensity averages c_1, c_2 are taken from Eq (20)), respectively.

Mostly in level sets or in active contours, it is often required to initialize the level set function to SDF (signed distance function) and avoid it to be too steep or too flat near the interface. In this regard, re-initialization is required to maintain the stability of level set function. In this paper, the Gaussian kernel is adapted, which not only removes the re-initialization but also avoids an expensive re-initialization of the level set function.

$$\phi(x, t=0) = \begin{cases} -\rho & x \in \Omega \setminus \partial\Omega \\ 0 & x \in \partial\Omega \\ \rho & x \in \Omega \setminus \Omega \end{cases} \quad (34)$$

$\rho \geq 0$ is a constant value, Ω_0 represents a region inside an initial contour, Ω is the image domain and $\partial\Omega$ is an initial contour. Finally, the iterative steps of the proposed method are summarized in following algorithm:

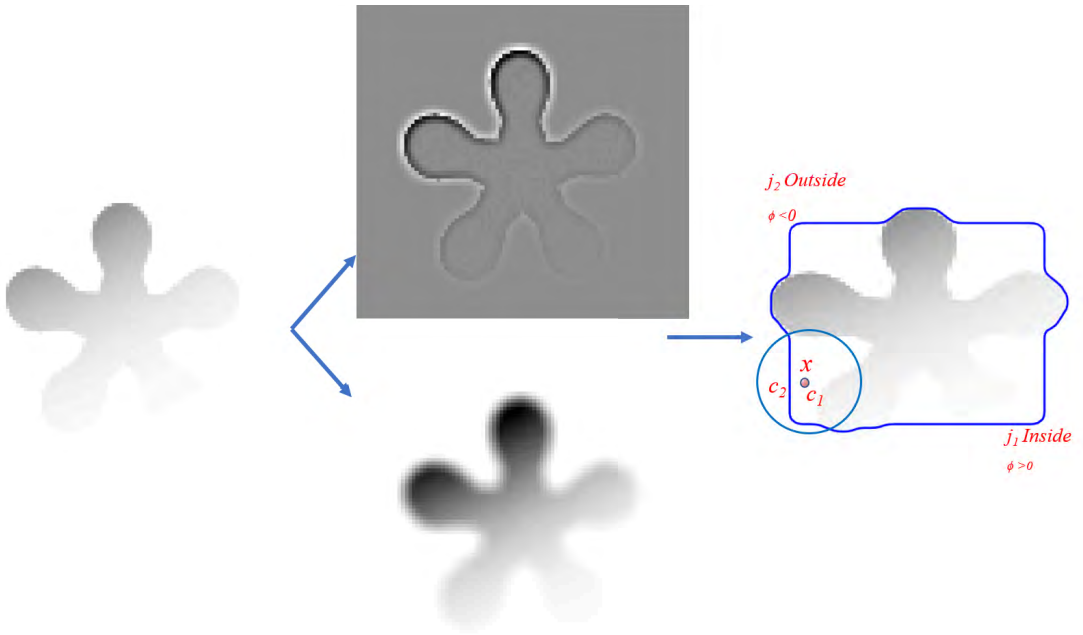

FIGURE 2. Visual representation of the proposed method. Original image (first column), bias field and correction (second column). Point x has been considered inside the circle locally. j_1,j_2 are global and c_1, c_2 are local means.

Algorithm 1 Iterative Algorithm for the Proposed Scheme

1) **Initialize** ϕ,$\phi(x, t = 0)$ from Eq (34).
2) $n = 1$.
3) **while** the solution is not converged **do**
4) Compute global intensity means from (6),
5) Compute the local intensity means from (20),
6) Compute the bias field from (19),
7) Solve ϕ using (33).
8) $n = n + 1$.
9) **end while**
10) **Output:** Final and accurate segmentation result, final ϕ.

IV. RESULTS

Every experiment of this paper executed in MATLAB on a Windows 10 environment installed in a PC with Intel core i7, 2.9 GHz with 16 GB RAM. The utilized parameters for proposed method are recorded in Table 1.

TABLE 1. Parameters used in the experiment and validation section.

Symbol	Quantity	Parameter value
α	Force term constant	100
υ	Length term constant	$0.00001 * 255 * 255$
σ	Gaussian kernel constant	0.5
ρ	Initial level set constant	1
ϵ	Dirac constant	1.5
∇	Time-step	0.1
w	w constant	0.9999
μ	p-Laplace regularization constant	1.5

The first experiment is shown in Fig 3, where we show the result of the proposed method over intensity inhomogeneous image. The initial curve on original image shown in (a), the estimated bias field and the corrected image is shown in (b), (c) and the result of the proposed method is shown in (d).

We obtain some more results and its comparison on images corrupted by intensity inhomogeneity in Fig 4, where original images with initial contours are shown in the first column, next columns show the results of the Chan-Vese [6], LBF [12], LIF [14], VLSBCS [23], [26], Zhang et al. [25] model and proposed method respectively. Results show that proposed method outperforms the previous state of art methods. In Table 2, We have calculated the time and iterations of each method based on Fig 4. It can be deduced from Table 2

TABLE 2. CPU time(in seconds) and iterations consumed by each method in Fig 4.

Methods		Circle	Star	T shape
Chan-Vese [6]	Iterations	**20**	**20**	**20**
	CPU time(sec)	**4.726**	**3.060**	**4.260**
LBF [12]	Iterations	50	50	50
	CPU time(sec)	13.643	9.783	7.637
LIF [14]	Iterations	500	500	500
	CPU time(sec)	18.071	5.847	6.0673
VLSBCS. [23]	Iterations	20	40	40
	CPU time(sec)	4.231	5.847	6.528
Zhang et al. [25]	Iterations	100	100	100
	CPU time(sec)	17.631	7.9663	7.526
Proposed method	Iterations	100	100	100
	CPU time(sec)	5.773	3.188	5.285

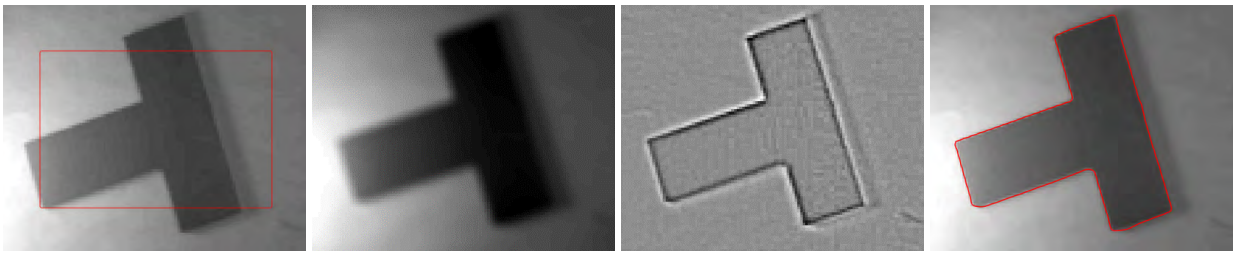

FIGURE 3. Image segmentation using proposed method over intensity inhomogeneous images a: Initialization. b: Bias field. c: Bias correction. d: segmentation result.

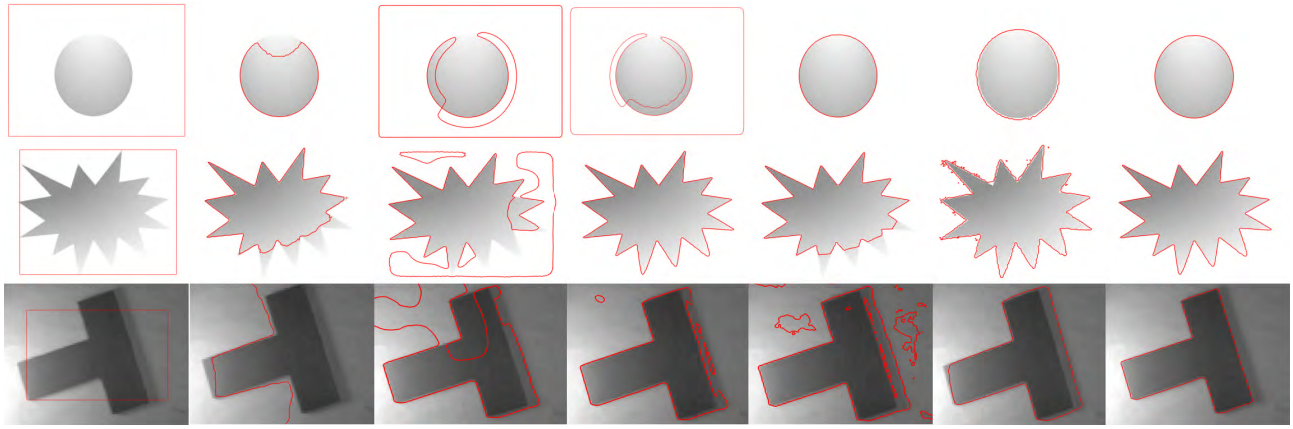

FIGURE 4. Proposed method on images having different intensity variation. second column (Chan-Vese [6]), third column (LBF [12]), fourth column (LIF [14]), fifth column (VLSBCS [23], [26]), sixth column Zhang et al. [25] and seventh column (proposed method) respectively.

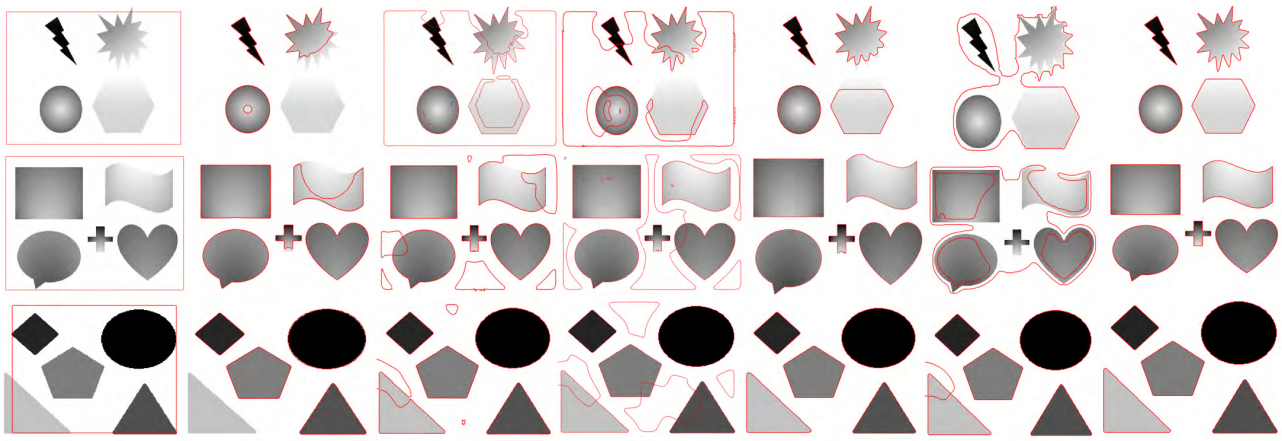

FIGURE 5. Proposed method results using images with multiple objects. second column (Chan-Vese [6]), third column (LBF [12]), fourth column (LIF [14]), fifth column (VLSBCS [23], [26]), sixth column (Zhang et al. [25]) method and seventh (proposed method) respectively.

that Chan-Vese consumed less time and iterations compared to previous methods, however, this method is not capable to yield accurate results. Proposed method on the other have produced accurate results with second least number of iterations and time.

Fig 5 shows some more intensity inhomogeneous images having multiple objects with intensity variation in foreground and background. Original images with initial contour are shown in the first column followed by the results of the Chan-Vese [6], LBF [12], LIF [14], VLSBCS [23], [26], Zhang et al. [25] and proposed method in column two, three, four, five, six and seven respectively. Results clearly specify the weaknesses of the previous methods, where Chan-Vese method is unable to get segmentation result in the presence of inhomogeneity, LBF and LIF methods are sensitive to initial position of the contour therefore these method yield inaccurate segmentation results. VLSBCS method performed well and yield accurate results in some cases, Zhang et al. [25]

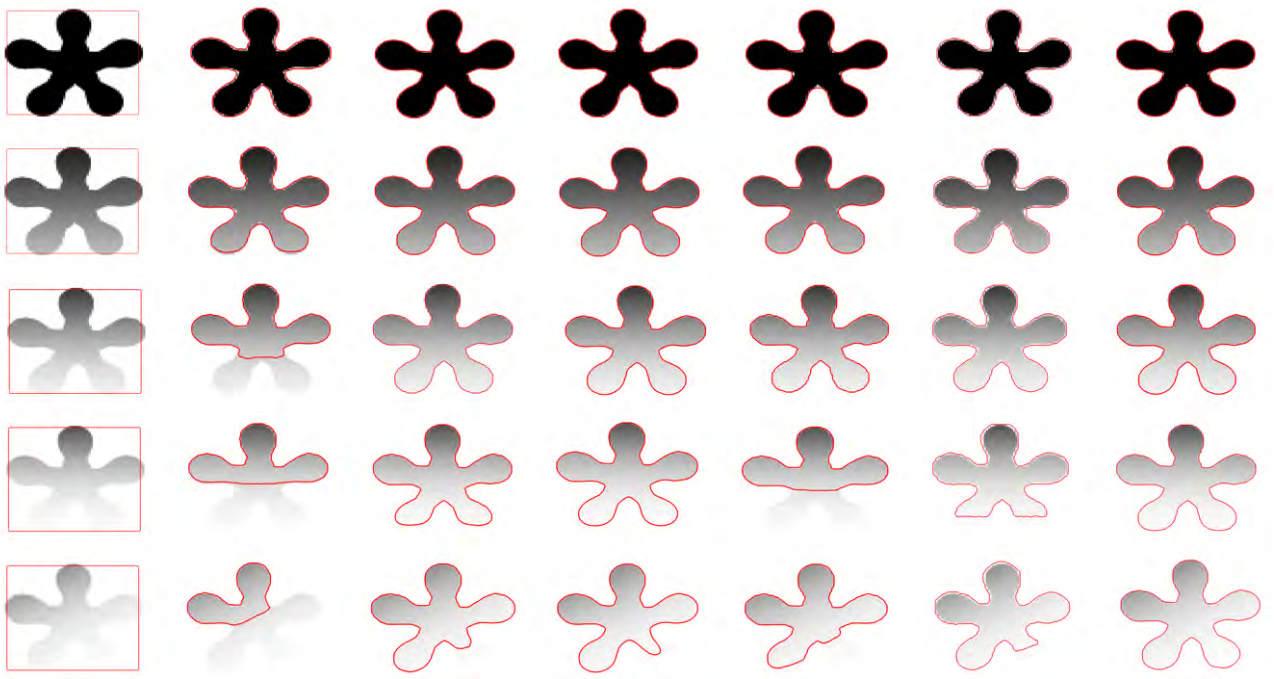

FIGURE 6. Proposed method using same image with different levels of intensity inhomogeneity. second column (Chan-Vese [6]), third column (LBF [12]), fourth column (LIF [14]), fifth column (VLSBCS [23], [26]), sixth column Zhang et al. [25] and seventh column (proposed method) respectively.

does not work well in the case of multiple object segmentation. on the other hand, proposed method has outperformed previous methods and achieved the required segmentation results correctly.

CPU time and number of iterations measured for Fig 5 are shown in Table 3, where Chan-Vese [6] did not yield accurate results but consumed least time and iterations. However, proposed method consumed less number of iterations and CPU time compared to previous method except Chan-Vese [6] and produced accurate results.

TABLE 3. CPU time(in seconds) and iterations consumed by each method in Fig 5.

Methods		row 1	row 2	row 3
Chan-Vese [6]	Iterations	**20**	**20**	**20**
	CPU time(sec)	**8.548**	**3.711**	**2.936**
LBF [12]	Iterations	50	50	50
	CPU time(sec)	12.464	12.645	9.602
LIF [14]	Iterations	500	500	500
	CPU time(sec)	18.237	19.304	8.286
VLSBCS. [23]	Iterations	100	200	200
	CPU time(sec)	22.939	43.141	14.830
Zhang et al. [25]	Iterations	200	200	400
	CPU time(sec)	21.177	28.776	214.852
Proposed method	Iterations	50	50	100
	CPU time (sec)	10571	6.411	3.859

In Fig 6, the same image is used with a different level of intensity inhomogeneity. Results and its comparisons are demonstrated in second column (Chan-Vese [6]), third column (LBF [12]), fourth column (LIF [14]), fifth column (VLSBCS [23], [26]), sixth column (Zhang et al. [25]) and seventh column (proposed method) respectively. Results show that as the level of inhomogeneity increases the previous methods give up and perform inaccurate segmentation, while proposed method maintains its stability and perform accurate segmentation.

We have measured CPU time and iterations of each method in Table 4 based on Fig 6. The performance of the proposed

TABLE 4. CPU time(in seconds) and iterations consumed by each method in Fig 6.

Methods		row 1	row 2	row 3	row 4	row 5
Chan-Vese [6]	Iterations	20	20	20	20	20
	CPU time(sec)	1.548	1.711	1.936	1.711	2.936
LBF [12]	Iterations	20	20	20	30	50
	CPU time(sec)	3.780	3.690	3.643	5.184	8.296
LIF [14]	Iterations	500	500	500	500	700
	CPU time(sec)	2.694	2.865	2.744	2.676	3.562
VLSBCS. [23]	Iterations	50	50	50	200	200
	CPU time(sec)	1.987	2.030	1.967	5.572	5.538
Zhang et al. [25]	Iterations	50	100	100	150	150
	CPU time(sec)	4.155	14.786	12.579	22.332	27.355
Proposed method	Iterations	20	30	30	70	70
	CPU time(sec)	1.047	1.148	1.346	1.604	1.912

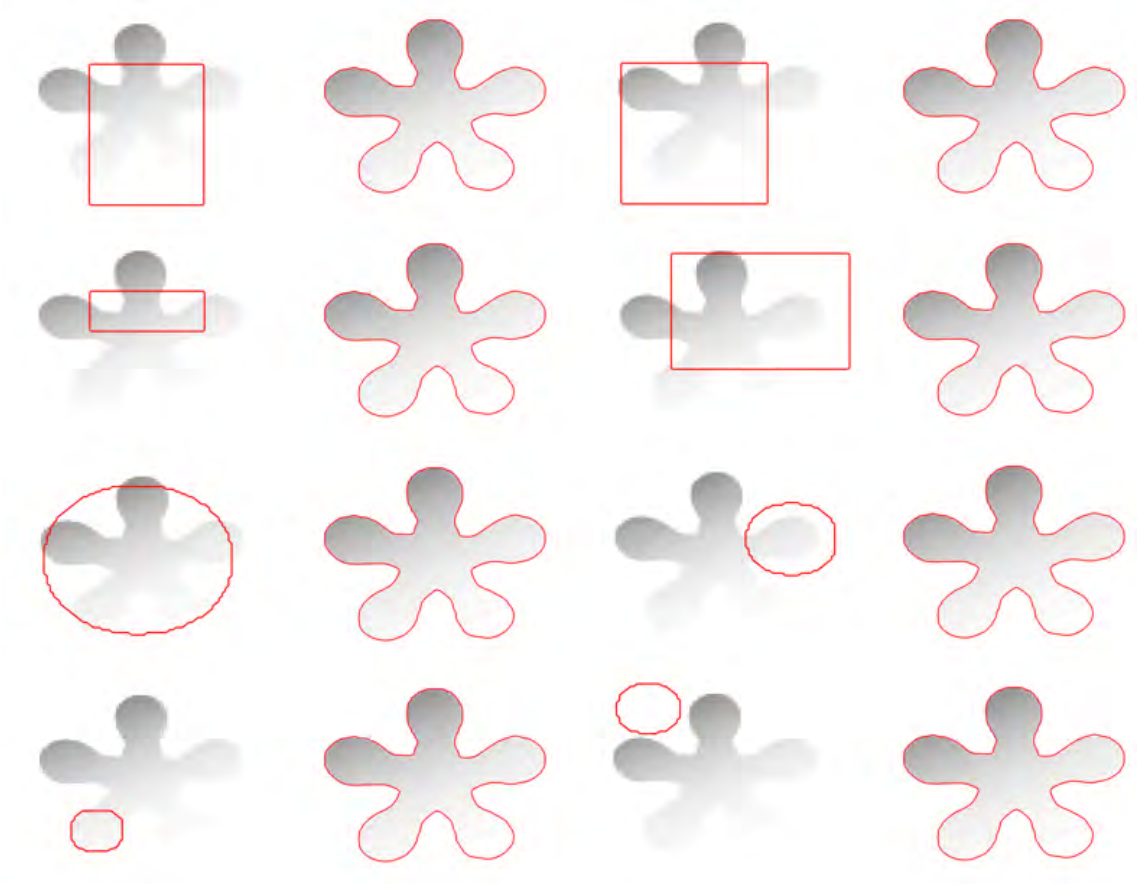

FIGURE 7. Proposed method result with different contour initializations. Square contour initialization: First and second row. Circular initialization: third and fourth row.

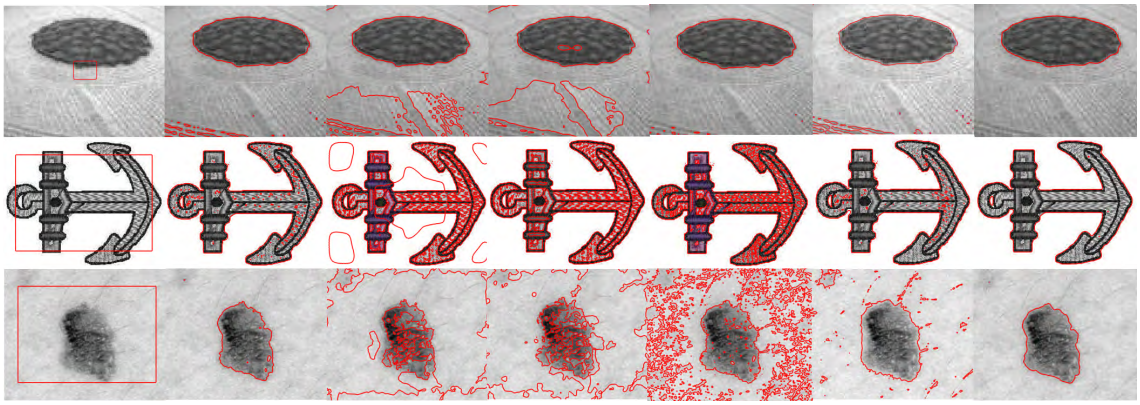

FIGURE 8. Result of the proposed method on textured images. second column (Chan-Vese [6]), third column (LBF [12]), fourth column (LIF [14]), fifth column (VLSBCS [23], [26]), sixth column Zhang et al. [25] and seventh column (proposed method) respectively.

method is conspicuous in terms of CPU time and iterations compared to previous methods.

Local region based methods [12] can handle intensity inhomogeneity to some extent however, these methods are very delicate to their initial position of the curve. Therefore, in order to validate the stability of the proposed method different initializations are used in Fig 7 including circular and squared shaped. The results show that proposed method yields accurate segmentation result regardless of different positions of the initial contour.

In Fig 8, three different textured images are taken in consideration. Results and its comparisons are demonstrated in second column (Chan-Vese [6]), third column (LBF [12]), fourth column (LIF [14]), fifth column (VLSBCS [23], [26]),

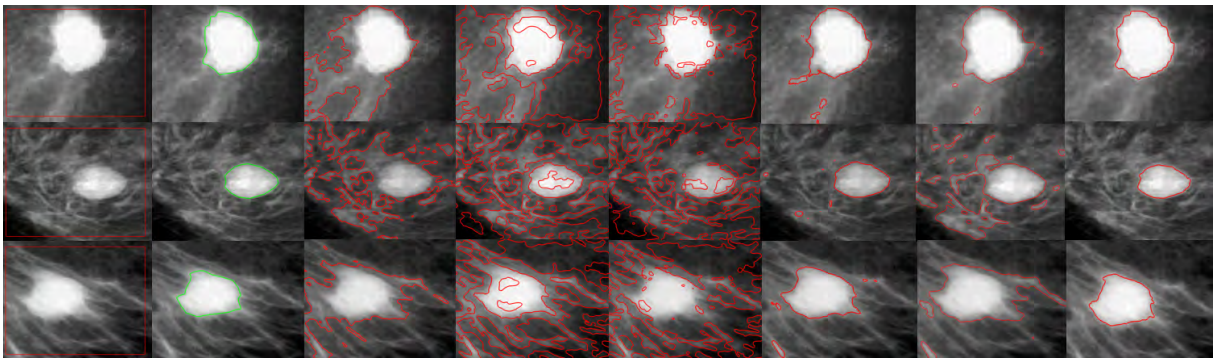

FIGURE 9. Quantitative comparison of the proposed method with previous methods. First column: Original Image with initialization. Second column: ground truth. Third column: Chan-Vese [6] result. Fourth column: LBF [12] result. Fifth column: LIF [14] result. Sixth column: [23] result. Seventh column: Zhang et al. [25]: Eighth column Proposed method result.

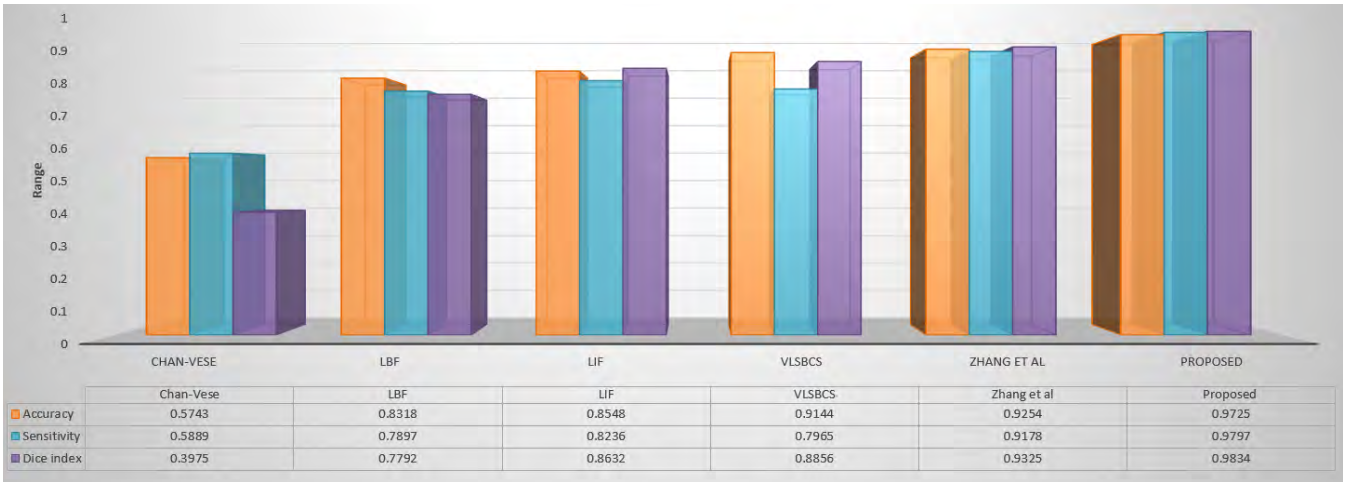

	Chan-Vese	LBF	LIF	VLSBCS	Zhang et al	Proposed
Accuracy	0.5743	0.8318	0.8548	0.9144	0.9254	0.9725
Sensitivity	0.5889	0.7897	0.8236	0.7965	0.9178	0.9797
Dice index	0.3975	0.7792	0.8632	0.8856	0.9325	0.9834

FIGURE 10. Quantitative analysis of the proposed method.

sixth column (Zhang et al. [25]) and seventh column (proposed method) respectively. Results demonstrate that proposed method has produced better results compared to previous methods.

V. QUANTITATIVE COMPARISONS

For quantitative comparison, we perform segmentation on mammogram images in Fig 9 taken from the mini-MIAS database [29]. In Fig 9, initial images and initial contours are shown in column 1, ground truths are shown in column2 followed by the results of the Chan-Vese [6], LBF [12], LIF [14], VLSBCS [23] and proposed method in column 3,4,5,6 and 7 respectively. Regardless of complex intensity variations, proposed method achieves its goal and obtain segmentation results correctly. Moreover, we compute the accuracy, sensitivity and Dice metric values to compare our method quantitatively. The obtained result will be considered as good when the measured values of these metrics are close to 1. Accuracy metric refers to closeness of segmented region to ground truth region, sensitivity metric value defines that all detected regions (tumors) are correct and belongs to the ground truth Dice coefficient measure how much detected tumor region overlaps the ground truth. These metrics are defined as:

$$Accuracy = \frac{TP + TN}{TP + TN + FP + FN}, \tag{35}$$

$$DSC = \frac{2 \times TP}{2 \times TP + FP + FN} \tag{36}$$

$$Sen = \frac{TP}{TP + FN} \tag{37}$$

where TP (true positive)corresponds to segmented tumor tissues, TN (true negative) corresponds to correctly unsegmented regions, FP (false positive) corresponds to the normal regions considered as tumor regions and FN (false negative) corresponds to the undetected tumor regions, respectively.

Fig 10 shows the validation metrics analysis and it shows that proposed method has achieved better result compared to previous methods.

We have also measured the average CPU time and average number of iterations of each method on mammogram images taken from [29] database in Table 5. Table shows that proposed method and Chan-Vese method consume less number

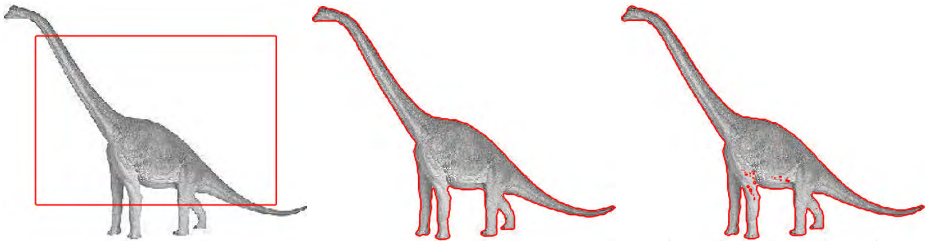

FIGURE 11. Effect of p-Laplace length regularization term a: Initialization b: Segmentation result with p-Laplace term. c: Segmentation result without p-Laplace term.

of iterations and CPU time, however, Chan-Vese method is unable to get desired results. Proposed method, on the other hand, achieved the desired results smoothly.

TABLE 5. Average CPU time and Iterations of each method.

Methods	Average CPU time	Average number of Iterations
Chan-Vese [6]	4.301	30
LBF [12]	10376	50
LIF [14]	11.255	500
VLSBCS [23]	11.466	50
Zhang et al. [25]	6.568	50
Proposed	4.7813	50

VI. DISCUSSION

Existing local region based active contour methods are insufficient to segment inhomogeneous objects properly. Proposed method incorporated the advantages of the previous methods and formulated a new modified method. With the consideration of the bias field estimation inside of the fitted image model, the proposed method has significantly improved its performance.

A. PARAMETER w AND μ

The parameter w and μ have a vital role during level set minimization. w parameter handles the amount of local force required to handle inhomogeneities inside an image. Parameter μ has been taken into consideration and its value is chosen between 1 and 2 respectively. This parameter provides smooth contours by avoiding the occurrence of unnecessary contours and holding the curve not to pass through fuzzy boundaries.

B. p-LAPLACE REGULARIZATION EFFECT

The existence of p-Laplace regularization term helps to converge the level set smoothly. Besides, it also helps to avoid the occurrence of unimportant contours during curve minimization. This can be seen in Fig 11, where Fig 11(a) is showing the initial curve, Fig 11(b) and Fig11(c) showing the result of proposed method with p-Laplace and without p-Laplace length regularization.

VII. CONCLUSION

In this paper, we have proposed a novel active contour model based on the combination of the local and global fitted image models for intensity inhomogeneous image segmentation. Local region model acquires bias field information into a level set formulation, which increases the efficiency of the proposed method. LBF [12] and Chan-Vese [6] model intensity means are formulated in a fitted image model and integrated with bias field, which overcome the limitations of previous local and global region based methods. Furthermore, the proposed method uses a scaled p-Laplace integral length regularization term, which overcome the problems of the previous regularization and restricts the contour to object boundary. Finally, the Gaussian filter is adapted to regularize the level set and to avoid an expensive reinitialization. We have performed several experiments on images with different intensity variation. For quantitative validation, we use accuracy, sensitivity and Dice index metric analysis. Results section show that proposed method gets high accuracy, sensitivity and Dice index values compared to previous methods.

REFERENCES

[1] A. Elnakib, G. Gimel'farbJasjit, S. Suri, and A. El-Baz, "Medical image segmentation: A brief survey," in *Multi Modality State-of-the-Art Medical Image Segmentation and Registration Methodologies*. New York, NY, USA: Springer, 2011, pp. 1–39.
[2] M. Kass, A. Witkin, and D. Terzopoulos, "Snakes: Active contour models," in *Proc. 1st Int. Conf. Comput. Vis.*, vol. 259, 1987, p. 268.
[3] V. Caselles, R. Kimmel, and G. Sapiro, "Geodesic active contours," *Int. J. Comput. Vis.*, vol. 22, no. 1, pp. 61–79, 1997.
[4] C. Li, C. Xu, C. Gui, and M. D. Fox, "Level set evolution without re-initialization: A new variational formulation," in *Proc. IEEE Comput. Soc. Conf. Comput. Vis. Pattern Recognit. (CVPR)*, vol. 1, Jun. 2005, pp. 430–436.
[5] D. Mumford and J. Shah, "Optimal approximations by piecewise smooth functions and associated variational problems," *Commun. Appl. Math.*, vol. 42, no. 5, pp. 577–685, 1989.
[6] T. F. Chan and L. A. Vese, "Active contours without edges," *IEEE Trans. Image Process.*, vol. 10, no. 2, pp. 266–277, Feb. 2001.
[7] K. Zhang, L. Zhang, H. Song, and W. Zhou, "Active contours with selective local or global segmentation: A new formulation and level set method," *Image Vis. Comput.*, vol. 28, no. 4, pp. 668–676, 2010.
[8] S. Soomro, F. Akram, J. H. Kim, T. A. Soomro, and K. N. Choi, "Active contours using additive local and global intensity fitting models for intensity inhomogeneous image segmentation," *Comput. Math. Methods Med.*, vol. 2016, Sep. 2010, Art. no. 9675249.
[9] S. Soomro, A. Munir, and K. N. Choi, "Hybrid two-stage active contour method with region and edge information for intensity inhomogeneous image segmentation," *PLoS ONE*, vol. 13, no. 1, p. e0191827, 2018.

[10] A. Munir, S. Soomro, C. H. Lee, and K. N. Choi, "Adaptive active contours based on variable kernel with constant initialization," *IET Image Process.*, vol. 12, no. 7, pp. 1117–1123, Feb. 2018.
[11] S. Soomro, F. Akram, A. Munir, C. H. Lee, and K. N. Choi, "Segmentation of left and right ventricles in cardiac MRI using active contours," *Comput. Math. Methods Med.*, vol. 2017, Aug. 2017, Art. no. 8350680.
[12] C. Li, C.-Y. Kao, J. C. Gore, and Z. Ding, "Minimization of region-scalable fitting energy for image segmentation," *IEEE Trans. Image Process.*, vol. 17, no. 10, pp. 1940–1949, Oct. 2008.
[13] L. Wang, L. He, A. Mishra, and C. Li, "Active contours driven by local Gaussian distribution fitting energy," *Signal Process.*, vol. 89, pp. 2435–2447, Dec. 2009.
[14] K. Zhang, H. Song, and L. Zhang, "Active contours driven by local image fitting energy," *Pattern Recognit.*, vol. 43, no. 4, pp. 1199–1206, Apr. 2010.
[15] Y. Peng, F. Liu, and S. Liu, "Active contours driven by normalized local image fitting energy," *Concurrency Comput., Pract. Exper.*, vol. 26, pp. 1200–1214, Apr. 2014.
[16] X. Xie, A. Zhang, and C. Wang, "Local average fitting active contour model with thresholding for noisy image segmentation," *Optik-Int. J. Light Electron Opt.*, vol. 126, pp. 1021–1026, May 2015.
[17] X.-F. Wang, D.-S. Huang, and H. Xu, "An efficient local Chan–Vese model for image segmentation," *Pattern Recognit.*, vol. 43, no. 3, pp. 603–618, 2010.
[18] L. Wang, C. Li, Q. Sun, D. Xia, and C.-Y. Kao, "Active contours driven by local and global intensity fitting energy with application to brain MR image segmentation," *Comput. Med. Imag. Graph.*, vol. 33, pp. 520–531, Oct. 2009.
[19] X. Li, D. Jiang, Y. Shi, and W. Li, *BioMedical Engineering OnLine*, vol. 14. London, U.K.: BioMed Central, 2015, pp. 1–8.
[20] G. Liu, H. Li, and L. Yang, "A topology preserving method of evolving contours based on sparsity constraint for object segmentation," *IEEE Access*, vol. 5, pp. 19971–19982, 2017.
[21] H. Lv, Z. Wang, S. Fu, C. Zhang, L. Zhai, and X. Liu, "A robust active contour segmentation based on fractional-order differentiation and fuzzy energy," *IEEE Access*, vol. 5, pp. 7753–7761, 2017.
[22] S. Zhu, X. Bu, and Q. Zhou, "A novel edge preserving active contour model using guided filter and harmonic surface function for infrared image segmentation," *IEEE Access*, vol. 6, pp. 5493–5510, 2018.
[23] C. Li, R. Huang, Z. Ding, J. C. Gatenby, D. N. Metaxas, and J. C. Gore, "A level set method for image segmentation in the presence of intensity inhomogeneities with application to MRI," *IEEE Trans. Image Process.*, vol. 20, no. 7, pp. 2007–2016, Jul. 2011.
[24] K. Zhang, Q. Liu, H. Song, and X. Li, "A variational approach to simultaneous image segmentation and bias correction," *IEEE Trans. Cybern.*, vol. 45, no. 8, pp. 1426–1437, Aug. 2015.
[25] K. Zhang, L. Zhang, K.-M. Lam, and D. Zhang, "A level set approach to image segmentation with intensity inhomogeneity," *IEEE Trans. Cybern.*, vol. 46, no. 2, pp. 546–557, Feb. 2016.
[26] C. Li, R. Huang, Z. Ding, C. Gatenby, D. Metaxas, and J. Gore, "A variational level set approach to segmentation and bias correction of images with intensity inhomogeneity," in *Proc. Int. Conf. Med. Image Comput. Comput.-Assisted Intervent.* Berlin, Germany: Springer, 2008, pp. 1083–1091.
[27] B. Zhou and C.-L. Mu, "Level set evolution for boundary extraction based on a p-Laplace equation," *Appl. Math. Model.*, vol. 34, pp. 3910–3916, Dec. 2010.
[28] G. Aubert and P. Kornprobst, *Mathematical Problems in Image Processing: Partial Differential Equations and the Calculus of Variations*, vol. 147. Berlin, Germany: Springer, 2006.
[29] (2003). *The Mini-MIAS Database of Mammograms*. [Online]. Available: http://peipa.essex.ac.uk/info/mias.html

SHAFIULLAH SOOMRO received the B.E. degree from QUEST, Nawabshah, Pakistan, in 2008, the M.E. degree from MUET, Jamshoro, Pakistan, in 2014, and the Ph.D. degree in computer science from Chung-Ang University, Seoul, South Korea, in 2018. He is currently an Assistant Professor in computer science at the Quaid-e-Awam University of Engineering, Science and Technology (QUEST), Larkana, Pakistan. His research interests include motion tracking, object segmentation, and 3-D image recognition.

TOUFIQUE AHMED SOOMRO received the B.E. degree in electronic engineering from the Mehran University of Engineering and Science Technology, Pakistan, in 2008, and the M.Sc. degree in electrical and electronic engineering from University Technology PETRONAS, Malaysia, in 2014. He is currently pursuing the Ph.D. degree with the School of Computing and Mathematics, Charles Sturt University, Australia. His research interests include most aspects of image enhancement and image analysis for medical images. He is currently implementing software-based algorithm for the detection of eye-related disease.

KWANG NAM CHOI received the B.S. and M.S. degrees from the Department of Computer Science, Chung-Ang University, South Korea, in 1988 and 1990, respectively, and the Ph.D. degree in computer science from the University of York, U.K., in 2002. He is currently a Professor with the School of Computer Science and Engineering, Chung-Ang University, Seoul, South Korea. His research interests include motion tracking, object categorization, and 3-D image recognition.